International Journal of Engineering Research and Science & Technology

www.ijerst.org

ISSN : 2319-5991

Vol. 22 No. 1(s) (2026)



ijerst.editor@gmail.com

editor@ijerst.com

www.ijerst.com
© 2026 IJERST. All Rights Reserved
Peer Reviewed, Referred & Indexed Journal

Research Paper

Investigation on the Structural, Properties of substrate temperature of the SnO_2 Thin Film via Spray- Pyrolysis.

Dhirsing Naik[a], Padurnag Deshmukh[a]

[a]Department of Physics, Jijamata College of Science and Arts, Bhende, 414605,

MS, India

Address correspondence to E-mail: dhirsingnaik1@gmail.com

Abstract:

In this work, SnO_2 thin films were deposited on glass substrates by spray pyrolysis at 300 and 400 °C. The formation of a polycrystalline tetragonal rutile phase was confirmed by X-ray diffraction, with average crystallite sizes of ~15 nm and ~47 nm. The surface morphology growth on the glass substrate was examined using scanning electron microscopy. Their energy band gaps are determined from absorbance spectra. The function group was identified in SnO2, and its force constant and bond length were determined from FTIR spectra

Keywords: Thin film; Structure properties; Optical properties; Band gap; Functional Group

Highlight

- Facile, cost-effective spray pyrolysis is used to deposit a SnO_2 thin film.
- Different substrate temperatures lead to a change in the optical band gap from 3.4 to 3.6 V.

Introduction

Rapid industrialization and population growth have released large amounts of organic pollutants into water, raising serious environmental and health concerns. Among various treatment techniques, semiconductor-based photocatalysis has emerged as an effective and environmentally friendly approach for degrading organic contaminants, owing to its ability to harness light energy to drive oxidation–reduction reactions without producing secondary pollution **[1].** Methylene Blue (MB) is a widely used synthetic dye in the textile, biological, and medical industries; however, its widespread use and discharge into water bodies make it

a persistent, toxic, and hazardous environmental contaminant. MB is toxic, carcinogenic, and non-biodegradable, posing serious threats to human health and environmental safety when released into wastewater. It can reduce light penetration in water, inhibit photosynthesis, and disrupt aquatic ecosystems. Its presence in natural waters is linked to respiratory distress, nausea, skin irritation, and other adverse health effects in humans, and it can harm aquatic life even at low concentrations [2].

Various metal-oxide semiconductors, such as MoO_3, WO_3, TiO_2, ZnO, ZrO_2, and In_2O_3, have been explored for the photocatalytic degradation of organic pollutants. The SnO_2 offers several distinct advantages, making it a competitive choice for dye degradation. SnO_2 has a wide band gap (~3.6 eV), excellent chemical and thermal stability, and strong resistance to photocorrosion, enabling durable performance under prolonged irradiation without structural degradation [3]. These intrinsic properties contributed to efficient photocatalytic activity and reliable operation under sunlight compared with other MOS materials. Additionally, the high electron mobility of SnO_2 facilitates rapid separation and transport of photogenerated charge carriers, reducing electron–hole recombination and enhancing the generation of oxygen reactive species that drive dye decomposition. SnO_2 has also been widely reported to serve as an effective component in heterostructures or doped systems, further improving charge separation and broadening light absorption, thereby enhancing the degradation efficiency of dyes such as methylene blue under UV or visible light irradiation [4].

Among various fabrication methods, spray pyrolysis is a simple, low-cost, and scalable technique for depositing metal oxide thin films. This method enables precise control of film thickness, composition, and microstructure by adjusting deposition parameters, including precursor concentration, spray rate, carrier gas flow, and substrate temperature [5]. In particular, substrate temperature critically influences the nucleation and growth kinetics, crystallinity, morphology, and surface characteristics of SnO_2 thin films, which in turn govern their optical and photocatalytic behavior. For example, mixed TiO_2-SnO_2 films grown at around 350 °C exhibit enhanced photocatalytic degradation efficiency due to improved crystalline quality and phase formation [6]. At lower substrate temperatures, incomplete thermal decomposition of the precursor often yields poor crystallinity and high defect densities, promoting rapid electron–hole recombination and poor photocatalytic performance. Conversely, higher substrate temperatures can enhance crystallinity and grain growth but may

reduce active surface area through grain coalescence, thereby adversely affecting photocatalytic efficiency if not optimized [7]. Therefore, identifying an optimal substrate temperature is essential to balance crystallinity, surface area, and charge-carrier dynamics while maximizing photocatalytic efficiency. While several studies have examined the structural and optical properties of spray-deposited SnO_2 films, systematic investigations that directly correlate substrate temperature with photocatalytic activity remain limited, particularly for pure SnO_2 thin films [8]. Understanding how temperature-induced microstructural and electronic changes influence photocatalytic degradation efficiency is crucial for optimizing SnO_2-based photocatalysts.[9]

In this study, n-type SnO_2 exhibited the tetragonal rutile phase at 300, and 600 °C. It was prepared via the Spray Pyrolysis method. The prepared samples were characterized by X-ray diffraction (XRD), UV-visible spectroscopy, scanning electron microscopy (SEM), and Fourier transform infrared spectroscopy (FTIR). The substrate temperature strongly influenced the optimized optical band gap. Additionally, crystallite size and lattice strain were strongly correlated with the structural properties of the prepared samples. The photocatalytic activities of the samples were evaluated by degrading Methylene blue (MB. In the end, the mechanism of photocatalytic degradation of Methylene blue (MB) dyes at 300 and 400 °C under solar irradiation was analysed in detail.

Experimental details

Spray pyrolysis was used to deposit a thin tin oxide coating on a microslide glass substrate. The glass substrate was cleaned multiple times with double-distilled water, acetone, and ethanol, and sonicated for 15 minutes with each liquid.

Table 1. represents the synthesis of SnO_2 with the molar concentration as given.

Sr. No.	Spray Parameters	Parameter value
1	Substrate temperature	300, 400^0C
2	Substrate and nozzle distance	45 cm
3	Carrier gas air pressure	20 LPM
4	Solution spray rate	0.5 ml min^{-1}

According to a standard procedure, 20 mL of double-distilled water is measured using a graduated cylinder and mixed with 0.2 M stannous chloride dihydrate (SnCl2·2H2O) under

continuous stirring. After the dropwise addition of 5 mL of hydrochloric acid (HCl), the mixture becomes homogeneous. The prepared solution was then sprayed through a 0.1-mm spray-gun nozzle to produce fine droplets, with a 20-minute deposition period at substrate temperatures of 300, 400, 500, and 600°C. The spray rate was maintained at 0.5 mL min^{-1}, and the deposited thin films were allowed to cool to room temperature. The SnO_2 thin films were homogeneous and bright white across all samples throughout the experiment.

Characterization techniques.

The structural properties of the SnO_2-deposited thin films were characterized using a Bruker D8Advance X-ray diffractometer (XRD). The Cu Kα radiation (λ = 1.54056 Å) was used at a grazing angle of 10°, with a diffraction angle range of 10-90. The crystallite size was determined from the broadening of the corresponding X-ray spectral peaks using Debye-Scherrer's formula. The surface morphology of the as-deposited thin films was examined by scanning electron microscopy (SEM). The bond vibrations (bending and stretching) of the functional group were identified using FTIR spectroscopy. The Raman spectrum confirms the formation of the rutile-phase SnO_2. The PC-based UV-Vis spectrophotometer (Systronics model 119) was used to measure the films' optical transmittance, reflectance, and absorbance spectra from 200 nm to 999 nm, with a glass substrate used as a standard.

Results and discussion

Figure 1. shows the typical X-ray spectra at substrate temperature 300 and 400^0C have diffracted peaks attributed to the polycrystalline structure of well-known crystalline materials, confirming phase orientation, crystallization, crystallite size, macrostrains, and microstructural properties of the prepared SnO_2 thin film. The sharp, well-resolved peaks indicated SnO_2-300 prepared thin films were prepared via spray techniques. Strong diffracted peaks were observed at 26.56, 33.96, 37.75, 51.76, 64.92, and 65.9, corresponding to the crystal planes (110), (101), (200), (211), (310), and (112), respectively. The synthesized materials exhibited all spectral peaks, which matched JCPDS Card No. 41-1441[10]. All the peaks are quite sharp, indicating that the synthesized materials are highly crystalline, with a spacing of 11.07 nm. diffraction analysis reveals that the synthesized SnO_2 has a tetragonal lattice associated with the P42/m n m space group. The tetragonal lattice of SnO_2 is shown schematically in Figure. 1a. Tin atoms are located at the body center and corners of the crystal lattice. Each tin atom is coordinated to six oxygen atoms in an octahedral arrangement, producing the octahedron depicted[11]

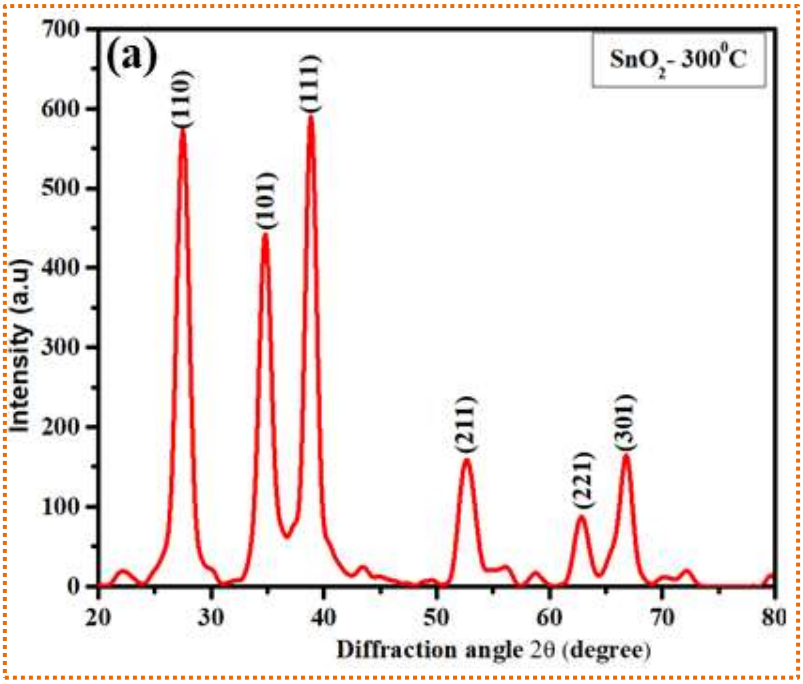


Figure 1. XRD diffraction spectra of SnO_2 at substrate temperatures (300^0C.

Table 2: Diffraction peak positions (2θ), Miller indices (hkl), FWHM (β) values, texture coefficient (TC), mean crystallite size (D), micro-strain (ε) values, a- and c-lattice constants belonging to SnO2 films deposited at varying temperatures

Table 2 Structure properties of the SnO_2 thin films

Sample	**a = b (Å)**	**c (Å)**	**V (Å)^3**	**FWHM**	**D (Å)**	**δ (/nm)^2 x 10^{14}**
SnO_2-300	4.751	3.185	71.7786	1.235	373.8	2.6

FTIR Spectroscopy of SnO_2

In figure 2. illustrated of the FTIR spectrum of the sample calcined at 300 °C exhibits several distinct absorption bands in the fingerprint region, indicating partial structural development. The band observed at 1081 cm^{-1} is attributed to asymmetric stretching vibrations of residual –OH groups or possible Sn–O–H bending modes, suggesting incomplete condensation and the presence of surface hydroxyl species[12]. The peak at 947 cm^{-1} corresponds to Sn–OH stretching or bridging Sn–O–Sn vibrations, reflecting partial network formation. The absorption band at 785 cm^{-1} is assigned to symmetric stretching vibrations of Sn–O–Sn linkages, whereas the prominent band at 450 cm^{-1} is characteristic of Sn–O lattice vibrations, confirming the formation of the metal–oxygen framework[13]. The persistence of hydroxyl-related bands at this temperature indicates incomplete crystallization

and retention of surface functional groups. In contrast, the FTIR spectrum of the sample calcined at 400 °C demonstrates noticeable structural evolution [14]. A significant reduction in the intensity of hydroxyl-associated bands is observed, indicating effective removal of surface –OH groups through thermal dehydration. Additionally, prominent absorption peaks appear at 609 cm^{-1} and 480 cm^{-1}, which are characteristic of Sn–O–Sn bridging vibrations and lattice stretching modes of crystalline SnO_2[15]. The disappearance or marked weakening of the bands at 1081 cm^{-1} and 947 cm^{-1} confirms enhanced condensation of the oxide network, leading to improved crystallinity and a more ordered SnO_2 structure. Overall, the spectral changes clearly indicate that increasing the calcination temperature from 300 °C to 400 °C facilitates structural densification, elimination of hydroxyl defects, and strengthening of the Sn–O lattice framework [16].

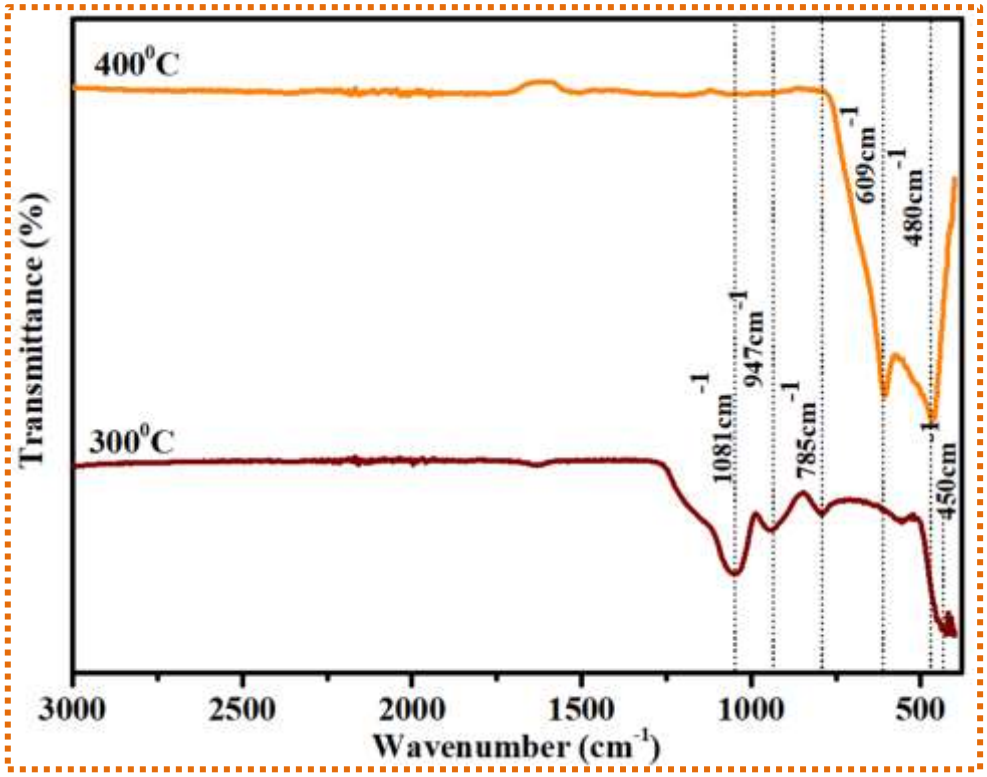


Figure 2. FTIR spectra of SnO_2 at substrate temperatures (300, and 400 °C).

The FTIR spectra of the samples annealed at 300 °C and 400 °C reveal the evolution of the metal–oxygen framework with temperature. The bands observed in the range 1053–425 cm^{-1} are attributed to stretching and bending vibrations of Sn–O and O–Sn–O bonds [17]. The sample annealed at 300 °C exhibits multiple broad absorption bands, indicating partial crystallization and structural disorder. In contrast, the 500 °C-annealed sample shows

fewer, sharper bands, confirming enhanced crystallinity and stabilization of the metal oxide lattice [18].

The absorbance spectra and their optical band gap

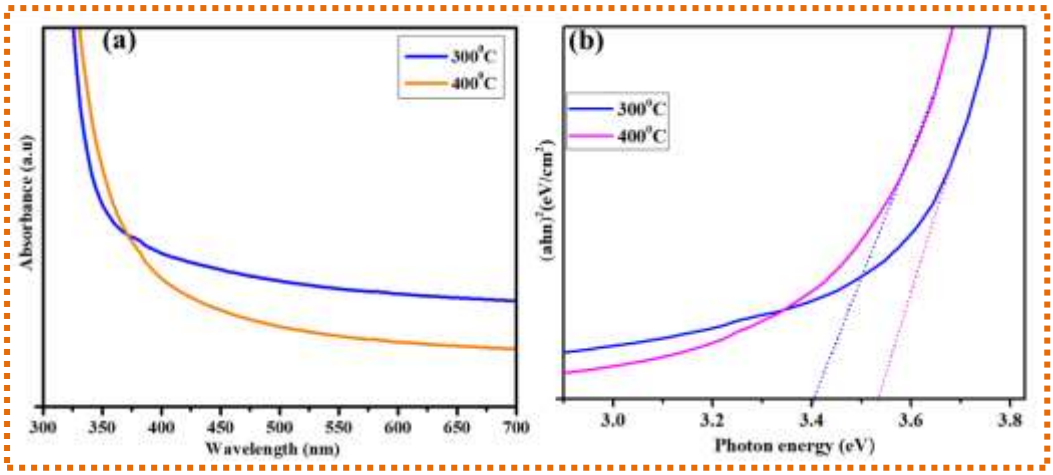


Figure 3. (a) absorbance spectra and (b) optical band gap spectra.

In figure 3. the diffuse absorption spectrum of the photon light interacts with the nanocrystalline SnO_2 -300 and SnO_2- 400 thin film, and transmittance, reflectance, and absorbance curves as a function of wavelength were analyzed using a UV-visible spectrophotometer [19]. First off, all converting the reflectance value (R) to absorbance using Beer-Lambert's law, and then the absorbance value is divided by the thickness of the prepared SnO_2 thin film to get the absorption coefficient (α) as a function of probing 200 nm to 999 nm wavelength [20].

$$\alpha = 2.303\left(\frac{A}{d}\right)$$

Beer- Lambert's law was used to investigate the absorption coefficient (α), a variation of Sn^+ molarity solution, where A is the optical absorbance and the thickness of SnO_2 materials. Further, it has been analysed optical band energies E_g with photon energies SnO_2 thin film values of diffuse reflectance R as equivalent of emission extinction coefficient,[F(R)], by using the Kubelka-Munk Method [21].

$$F(R) = \frac{\alpha}{S} = \frac{(1-R^2}{2R}$$

Also, DRS is analogous to Tau Plots derived from the Kubelka-Munk function, according to the above equation.

$$[ahv] = \beta_2(E - E_{g1})^2$$

$$[ahv] = \beta_2(E - E_{g2})^{1/2}$$

Where β_2 and β_2 are proportionality constants, an absorption coefficient as a function of photon energy (hv) and E_{g1}, E_{g2} is the optical band gap energy is direct (2) and indirect (1/2), respectively. **Figures 3(a, b).** show the dependence of the deposited SnO_2 thin film on photon energy for varying Sn+ molarity in solution [22]. The optical direct band gap energy was calculated as the intercept of a linear fit to the photon energy data extrapolated from the experimental data. It was discovered that the optical band gap energies went down as the Sn molarity in the SnO_2 thin film increased. As in the indirect band gap allowed band gap extrapolation portion (linear fit) versus photon energy, it has also been observed that the indirect optical band gap decreases [23]. The SnO2 thin film showed improved crystallinity and grain size, as well as a change in surface morphology. In the present work, the decrease in the optical band gap is attributed to oxygen-defect states (sub-gap absorption) and oxygen-vacancy states in the polycrystalline SnO2 thin film [24].

Conclusion

SnO_2 thin films deposition at different substrate temperatures (300-400°C) via a simple, low-cost-effective spray pyrolysis method. The structural, optical, morphological, and photocatalytic properties with deposition temperature. XRD analysis confirmed the formation of phase-pure tetragonal rutile SnO_2, with a progressive decrease in FWHM indicating improved crystallinity and reduced lattice defects at higher temperatures. The average crystallite size remained in the nanometer range, suggesting thermally stabilized crystal growth. Morphological studies revealed that particle size evolves with temperature, with greater uniformity and reduced size dispersion at higher temperatures. Optical analysis showed energy bandgap values ranging from 3.42 to 3.63 eV, while a systematic reduction in Urbach energy confirmed a decrease in structural disorder and an improvement in optical quality with increasing temperature.

Declarations

Ethics approval

All authors have read, understood, and complied as applicable with the statement on “Ethical responsibilities of Authors” as found in the Instructions for Authors.

Consent to participate

All authors have read, understood, and complied as applicable with the statement on "Consent to Participate" as found in the Instructions for Authors.

Consent for publication

All authors have read, understood, and complied as applicable with the statement on "Consent to Publish" as found in the Instructions for Authors.

Availability of data and material

The datasets generated during the current study are available from the corresponding author on reasonable request

Competing interests

We declare that this work has not been submitted for publication elsewhere, and we have no competing interests to report. All named authors have reviewed and approved the manuscript. Furthermore, we confirm that the order of authors listed in the manuscript has been agreed upon by all named authors.

Author contributions

Dhirsing Naik: Writing-original draft, Investigation, Formal analysis, graphs, software and Data curation;

Acknowledgements

The author is thankful to the Principal of Jijamata College of Science and Arts, Bhende.

References:

1. Zhu, D.; Zhou, Q. Action and Mechanism of Semiconductor Photocatalysis on Degradation of Organic Pollutants in Water Treatment: A Review. *Environ. Nanotechnol. Monit.Manag.***2019**,*11*,100255. https://doi.org/10.1016/j.enmm.2019.100255.
2. Wu, H.; Huang, B.; Qin, X.; Dai, Y. Recent Advances of Semiconductor Photocatalysis for Water Pollutant Treatment: Mechanisms, Materials and Applications. *Phys. Chem. Chem. Phys.* **2023**, *25*, 10210–10236. https://doi.org/10.1039/D3CP03391k.

3. Sun, Y.; O'Connell, D. W. Application of Visible Light Active Photocatalysis for Water Contaminants: A Review. *Water Environ. Res.* **2022**, *94*, e10781. https://doi.org/10.1002/wer.10781
4. Fujishima, A.; Zhang, X.; Tryk, D. A. Titanium Dioxide Photocatalysis and Related Surface Phenomena. Surf. Sci. Rep. 2008, 63, 515–582. https://doi.org/10.1016/j.surfrep.2008.10.001.
5. Batzill, M.; Diebold, U. The Surface and Materials Science of Tin Oxide. Prog. Surf. Sci. 2005, 79, 47–154. https://doi.org/10.1016/j.progsurf.2005.09.002.
6. Zhang, J.; Xu, Q.; Feng, Z.; Li, M.; Li, C. Importance of the Relationship between Surface Phases and Photocatalytic Activity of SnO_2. Angew. Chem. Int. Ed. 2008, 47, 1766–1769. https://doi.org/10.1002/anie.200704788.
7. Liu, B.; Zeng, H. C. Hydrothermal Synthesis of SnO_2 Nanostructures and Their Photocatalytic Properties. J. Am. Chem. Soc. 2003, 125, 4430–4431. https://doi.org/10.1021/ja0299905.
8. Chen, X.; Mao, S. S. Titanium Dioxide Nanomaterials: Synthesis, Properties, Modifications and Applications (General semiconductor photocatalysis mechanisms relevant to heterostructures). Chem. Rev. 2007, 107, 2891–2959. https://doi.org/10.1021/cr0500535
9. Effect of substrate temperature on structural, optical, and photocatalytic properties of TiO_2–SnO_2 mixed thin films, *Optical Materials* (2024) 116491. https://doi.org/10.1016/j.optmat.2024.116491
10. Batzill, M., & Diebold, U. (2005). The surface and materials science of tin oxide. *ProgressinSurfaceScience,79*(2–4),47–154. https://doi.org/10.1016/j.progsurf.2005.09.002.
11. Díaz-Guillén, J. A., et al. (2007). Structural and optical properties of SnO_2 thin films prepared by spray pyrolysis. *Thin Solid Films, 515*(24), 8764–8768. https://doi.org/10.1016/j.tsf.2007.03.123.
12. Pearton, S. J., Norton, D. P., Ip, K., Heo, Y. W., & Steiner, T. (2005). Recent progress in processing and properties of ZnO (for comparative oxide semiconductor discussion). *ProgressinMaterialsScience,50*(3),293340. https://doi.org/10.1016/j.pmatsci.2004.04.001.
13. Shannon, R. D. (1976). Revised effective ionic radii and systematic studies of interatomic distances in halides and chalcogenides. *Acta Crystallographic Section A, 32*(5),751–767. https://doi.org/10.1107/S0567739476001551.

14. Zhang, J., Xu, Q., Feng, Z., Li, M., & Li, C. (2008). Importance of the relationship between surface phases and photocatalytic activity of SnO_2. *Angewandte Chemie InternationalEdition,47*(9),1766–1769. https://doi.org/10.1002/anie.200704788.
15. Reddy, K. M., Manorama, S. V., & Reddy, A. R. (2003). Bandgap studies on anatase titanium dioxide nanoparticles. *Materials Chemistry and Physics, 78*(1), 239–245. https://doi.org/10.1016/S0254-0584(02)00343-7.
16. Díaz-Guillén, J. A., et al. (2007). Structural and optical properties of SnO_2 thin films prepared by spray pyrolysis. *Thin Solid Films, 515*(24), 8764–8768.* https://doi.org/10.1016/j.tsf.2007.03.123.
17. Sharma, R., & Khare, N. (2010). Size-dependent optical and structural properties of SnO_2 nanoparticles. *Journal of Physics D: Applied Physics, 43*(5), 055402. https://doi.org/10.1088/0022-3727/43/5/055402.
18. Tauc, J., Grigorovici, R., & Vancu, A. (1966). Optical properties and electronic structure of amorphous germanium. *Physica Status Solidi (b), 15*(2), 627–637. https://doi.org/10.1002/pssb.19660150224.
19. Zhang, J., Xu, Q., Feng, Z., Li, M., & Li, C. (2008). Importance of the relationship between surface phases and photocatalytic activity of SnO_2. *Angewandte Chemie International Edition, 47*(9), 1766–1769.* https://doi.org/10.1002/anie.200704788
20. Chen, X., & Mao, S. S. (2007). Titanium dioxide nanomaterials: Synthesis, properties, modifications, and applications. *Chemical Reviews, 107*(7), 2891–2959. https://doi.org/10.1021/cr0500535.
21. Liu, B., & Zeng, H. C. (2003). Hydrothermal synthesis of SnO_2 nanostructures and their photocatalytic properties. *Journal of the American Chemical Society, 125*(15), 4430–4431.https://doi.org/10.1021/ja0299905.
22. Cheng, H., et al. (2014). Oxygen vacancy promoted the photocatalytic activity of SnO_2 nanostructures. *Applied Catalysis B: Environmental, 147*, 434–441. https://doi.org/10.1016/j.apcatb.2013.09.021
23. Kaur, R., & Pal, B. (2012). Effect of fluorine doping on the photocatalytic activity of semiconductor oxides. *Applied Surface Science, 258*(24), 9725–9731. https://doi.org/10.1016/j.apsusc.2012.06.046
24. Houas, A., et al. (2001). Photocatalytic degradation pathway of methylene blue in water. *Applied Catalysis B: Environmental,31*(2),145–157. https://doi.org/10.1016/S0926-3373(00)00276-9